Electronic Supplementary Material (ESI) for Physical Chemistry Chemical Physics.

Supporting Information: Half Metallicity and Ferromagnetism of Vanadium Nitride Nanoribbons: A First-principles Study

Atish Ghosh,[†] Moumita Kar,[†] Chiranjib Majumder,[‡] and Pranab Sarkar[*,†]

Department of Chemistry, Visva-Bharati University, Santiniketan- 731235*, India, and Chemistry Division, Bhabha Atomic Research Centre, Mumbai* 400085*, India*

E-mail: pranab.sarkar@visva-bharati.ac.in

[*]To whom correspondence should be addressed
[†]Visva-Bharati University
[‡]Bhabha Atomic Research Centre

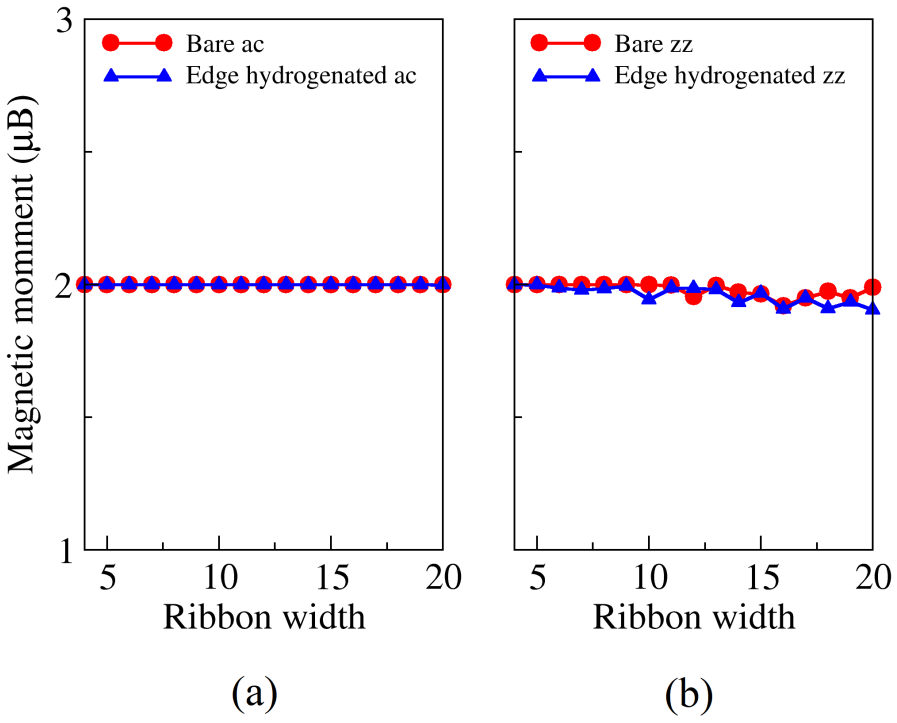

Figure S1: The magnetic momment (per VN pair) variation with width of the ribbons for bare and edge hydrogenated (a) ac and (b) zz VNNRs. The red lines are for bare NRs and the blue ones are for edge hydrogenated VNNRs.

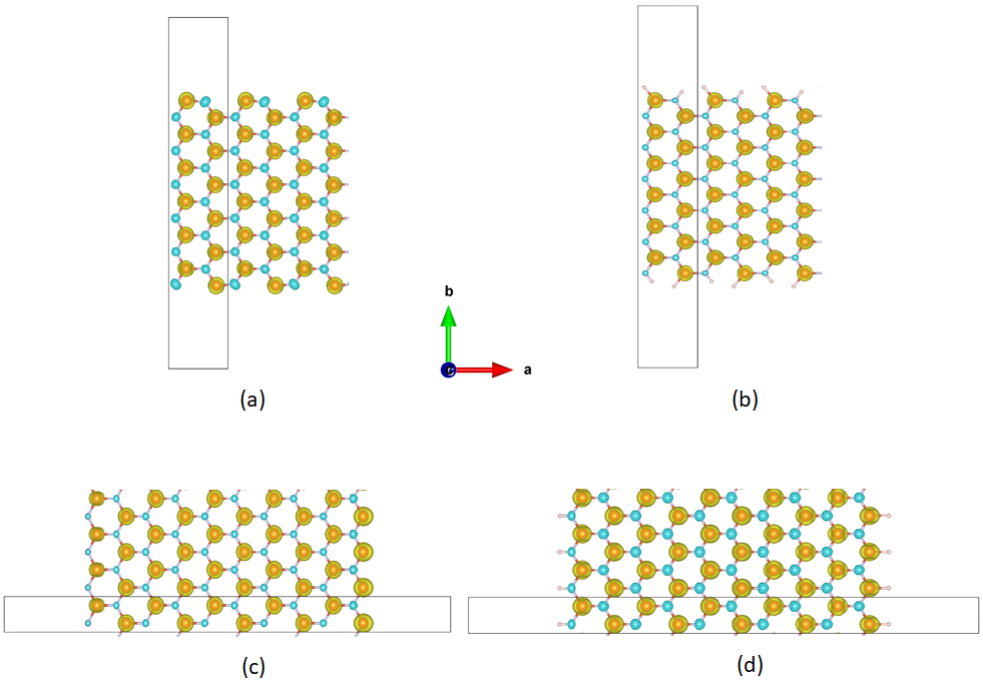

Figure S2: The spin density plots for (a) bare and (b) edge hydrogenated 12ac VNNR and (c) bare and (d) edge hydrogenated 10zz VNNR. The isosurface value os 0.025 e/Å^3.

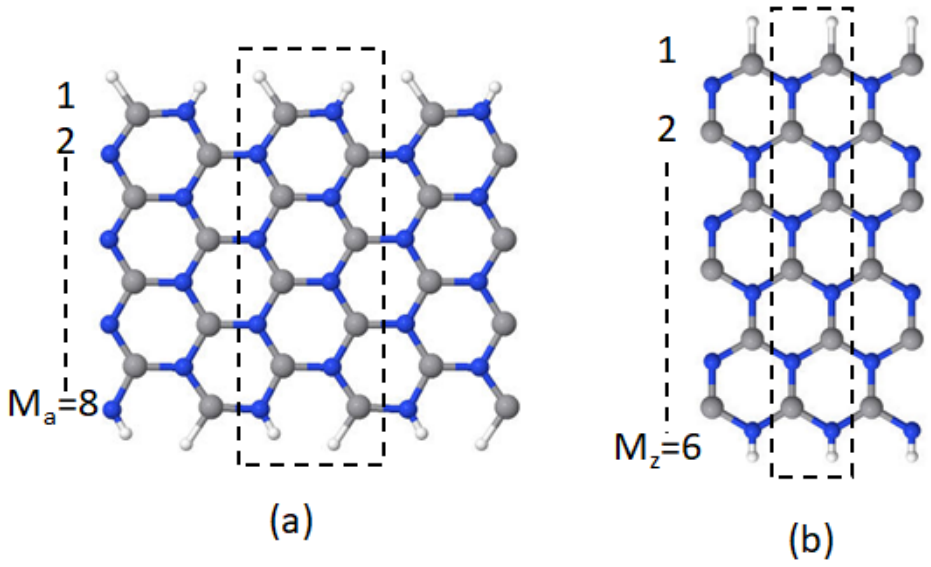

Figure S3: Optimized structure of edge hydrogenated (a) 8ac VNNR and (b) 6zz VNNR.

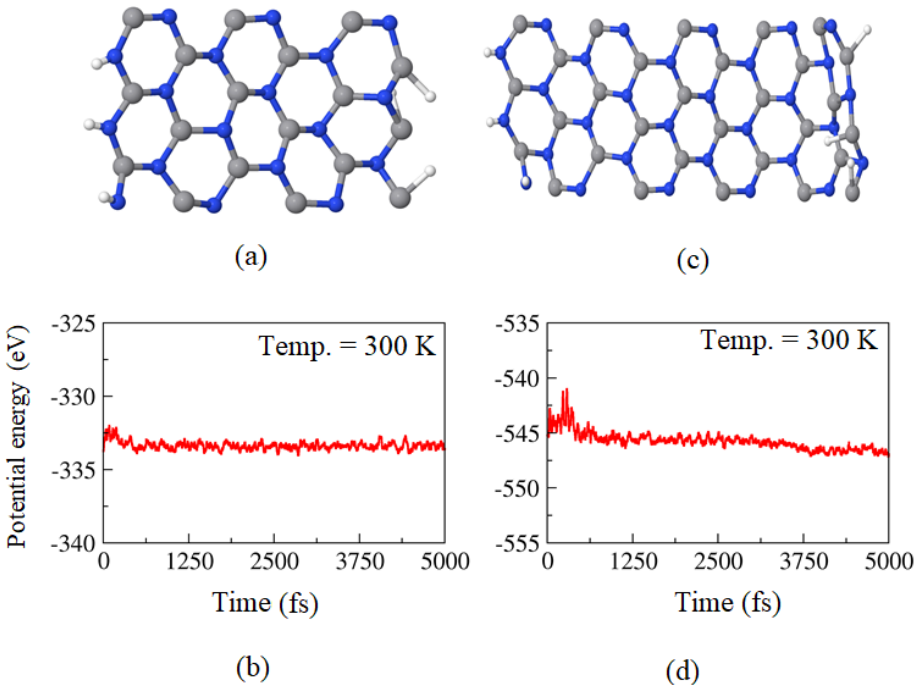

Figure S4: (a) Final structure and (b) total potential energy fluctuation of edge hydrogenated 6zz VNNR during AIMD simulation at 300 K. (c) Final structure and (d) total potential energy fluctuation of edge hydrogenated 10zz VNNR during AIMD simulation at 300 K.

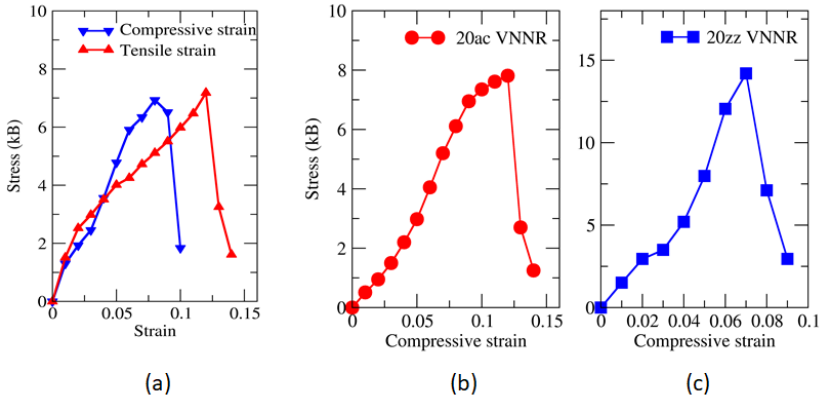

Figure S5: (a) The stress versus tensile and compressive strain for (1 × 2 × 1) supercell of edge hydrogenated 6zz VNNR. Stress versus compressive strain are plotted for edge hydrogenated (b) 20ac and (c) 20zz VNNRs.

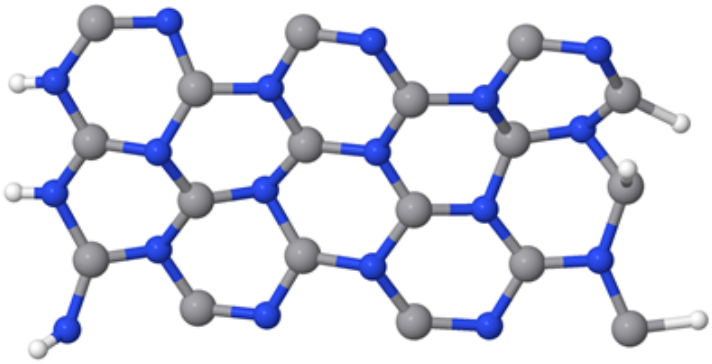

(a)

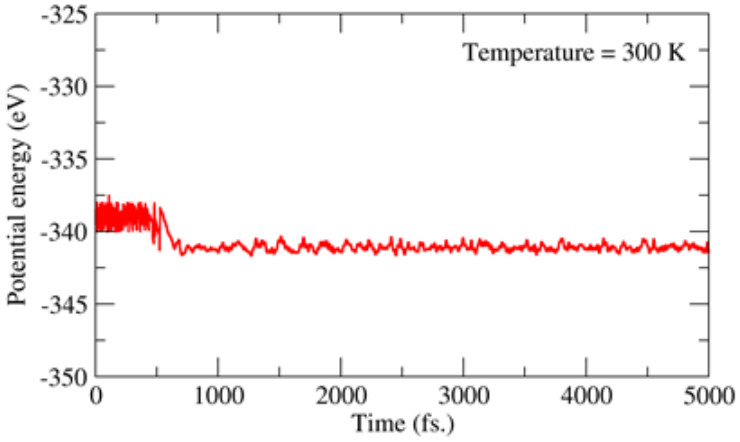

(b)

Figure S6: (a) Final structure and (b) total potential energy fluctuation of edge hydrogenated 6zz VNNR at 12% tensile strain during AIMD simulation at 300 K.

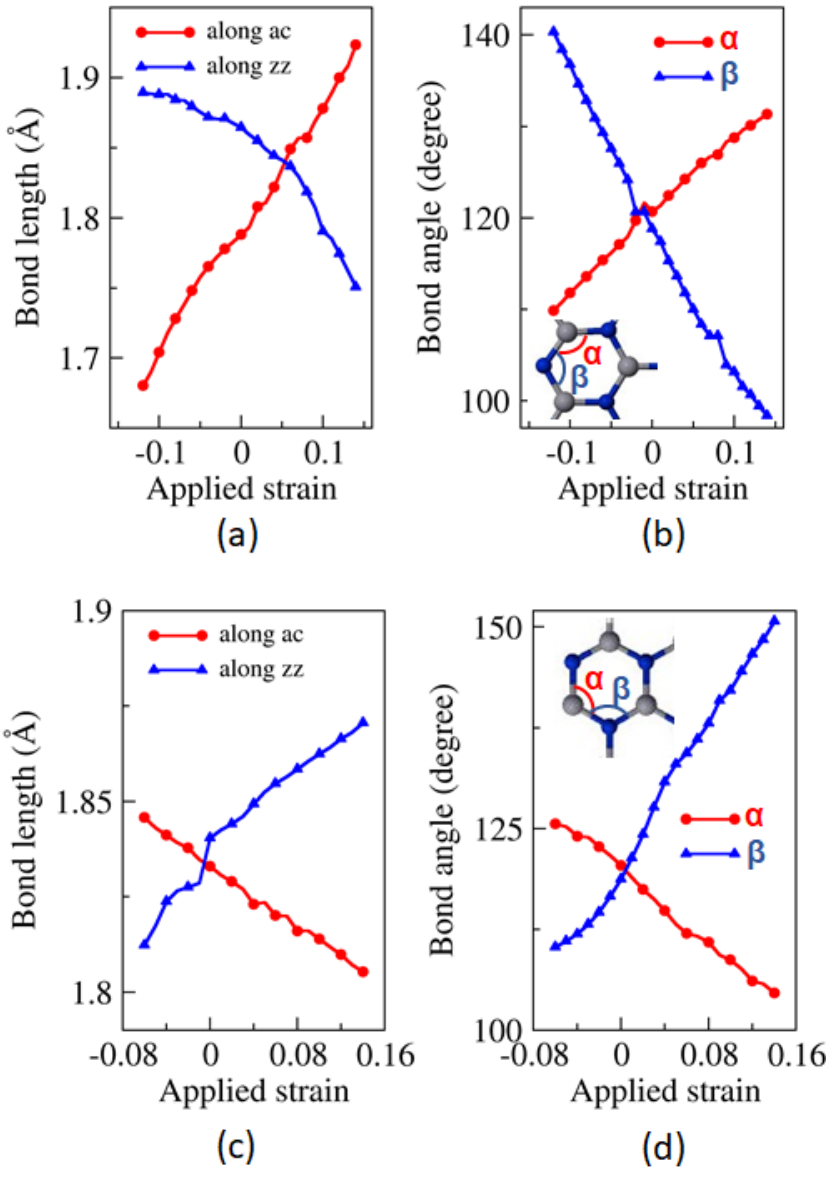

Figure S7: The variation of (a) bond length and (b) bond angle of edge hydrogenated 12ac VNNR with applied strain, and the variation of (c) bond length and (d) bond angle of edge hydrogetnated VNNR with applied strain.

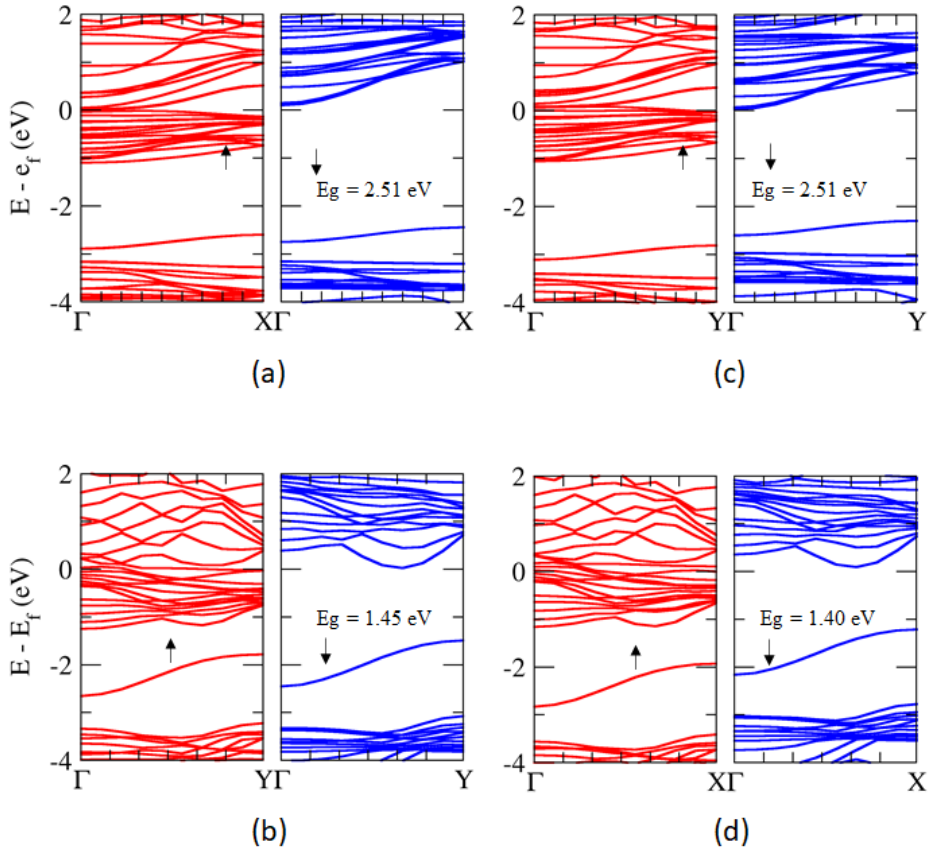

Figure S8: Band structure of edge hydrogenated (a) 8ac and (b) 6zz VNNR at GGA-PBE level of calculation compared with the band patterns of (c) 8ac and (d) 6zz VNNRs including the effect of spin orbit coupling (SOC) at the same level of calculation.

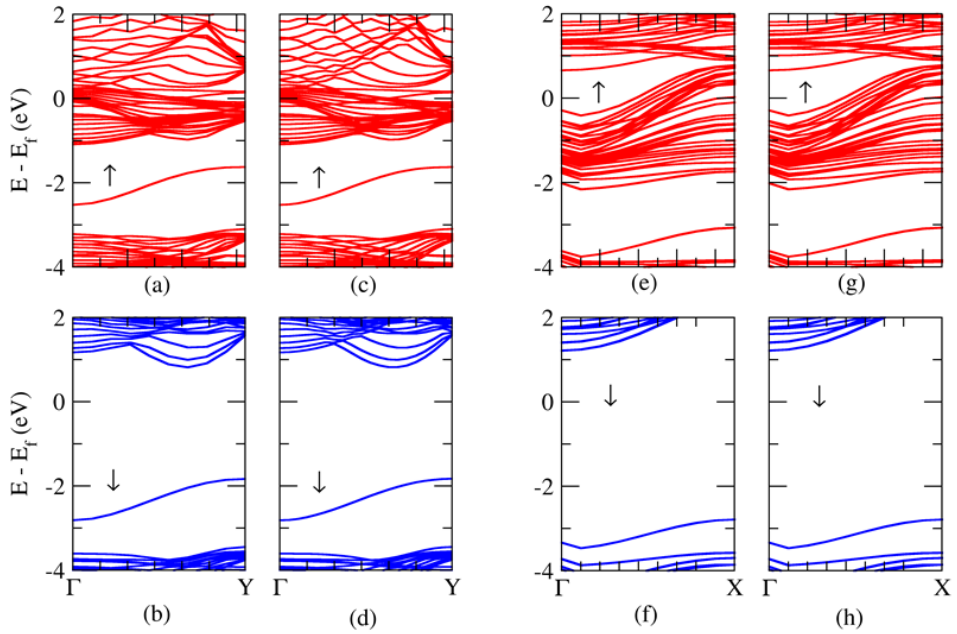

Figure S9: Band structure of edge hydrogenated 14zz VNNR with ($1 \times 10 \times 1$) kpoints. (a) and (b) for spin up and down respectively. (c) and (d) are the up and down spin band structures for the same structure with higher kpoints ($1 \times 15 \times 1$). Similarly, (e) and (f) are the band structure of edge hydrogenated 12ac VNNR with ($10 \times 1 \times 1$) kpoints where as (g) and (h) are the up and down spin band structures for the same structure with higher kpoints ($15 \times 1 \times 1$).

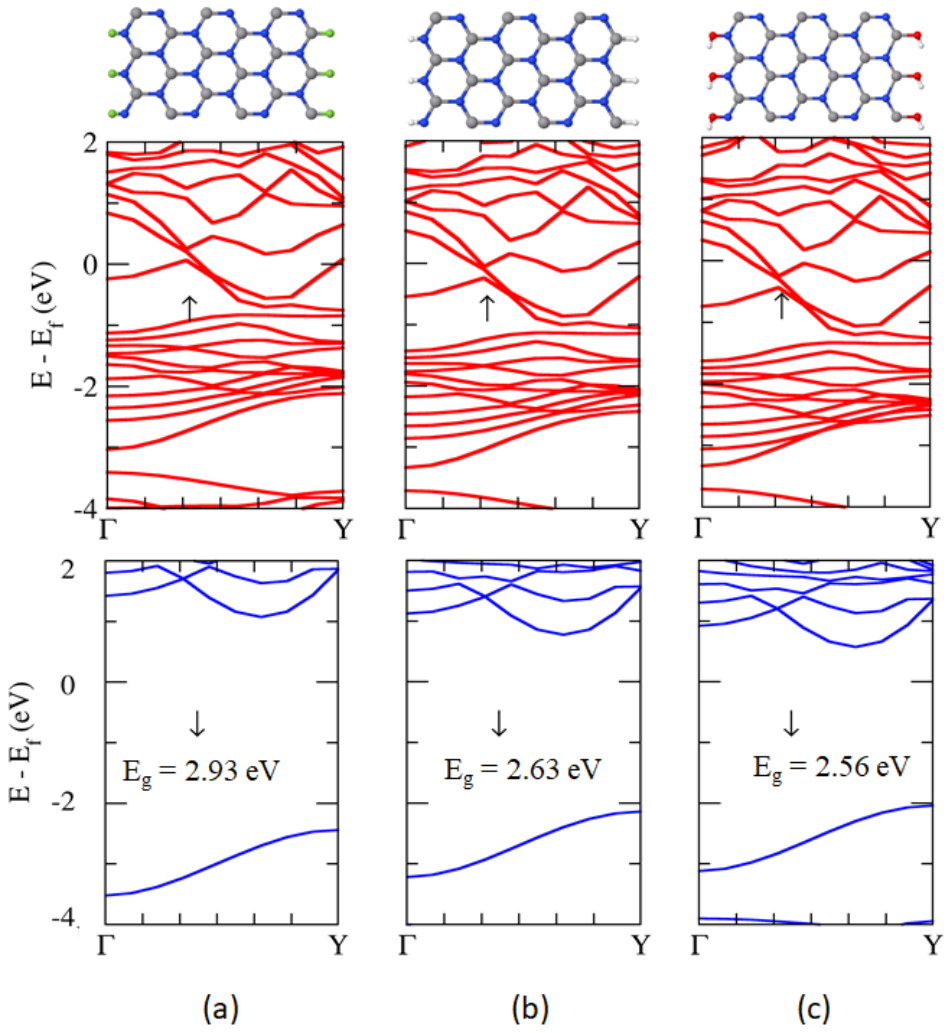

Figure S10: Spin resolved band structure (calculated at HSE06 level) of edge (a) F, (b) H, (c) OH passivated 6zz VNNR. Red lines signify up spin (↑) where blue ones signifies down spin (↓). Fermi energy level is shifted to zero.

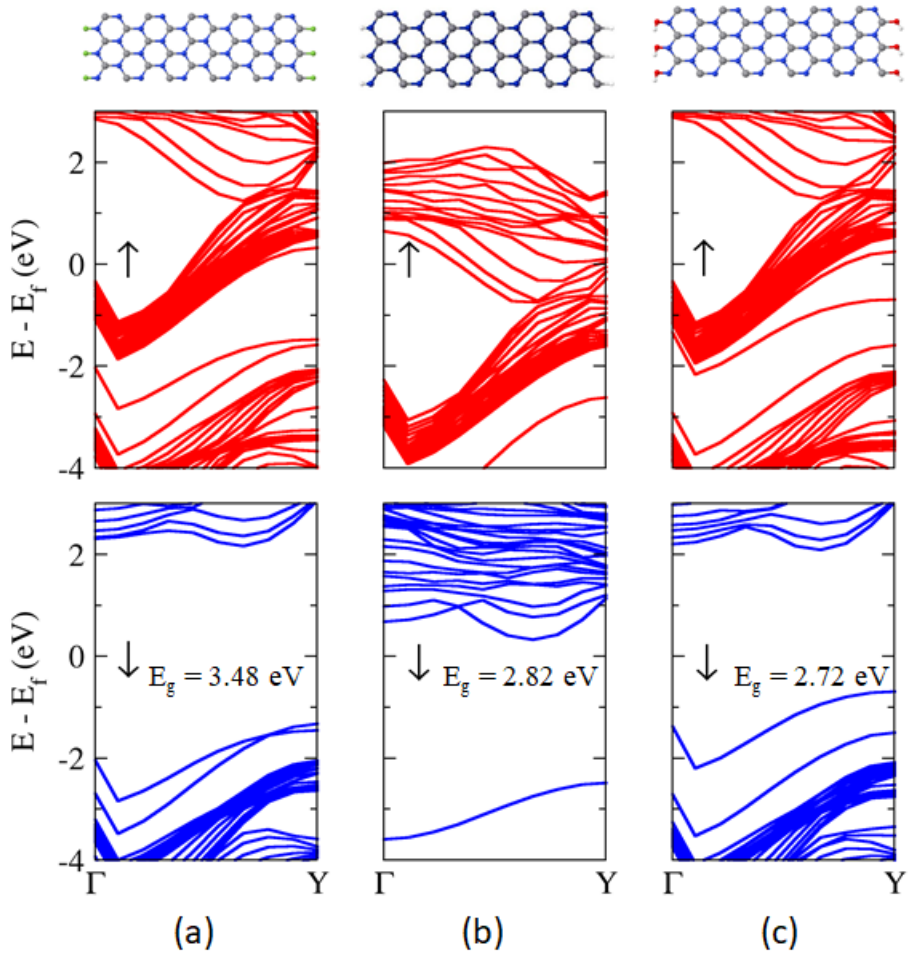

Figure S11: Optimized structures and spin resolved band structure (calculated at HSE06 level) of edge (a) F, (b) H, (c) OH passivated 10zz VNNR. Red lines signify up spin (↑) where blue ones signifies down spin (↓). Fermi energy level is shifted to zero.

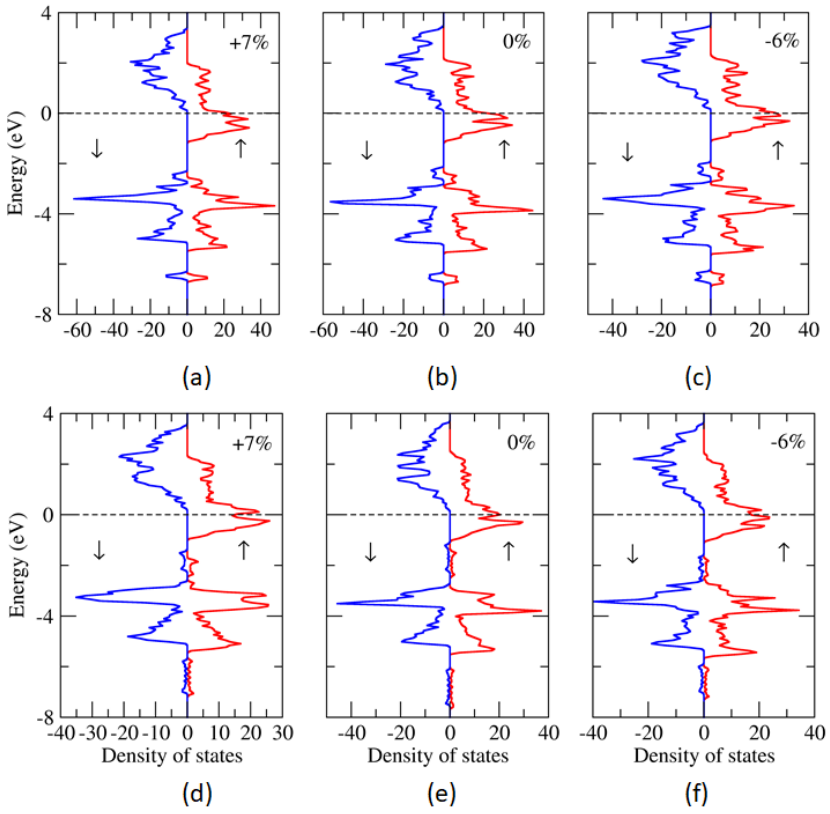

Figure S12: Density of states of edge hydrogenated 12ac VNNR at (a) 7% tensile strain, (b) 0% strain and (c) 6% compressive strain. Similarly, for the edge hydrogenated 10zz VNNR the density of states are plotted for (d) 7% tensile strain, (e) 0% strain and (f) 6% compressive strain. The red (↑) and blue curves (↓) are the DOS for up and down spin respectively.

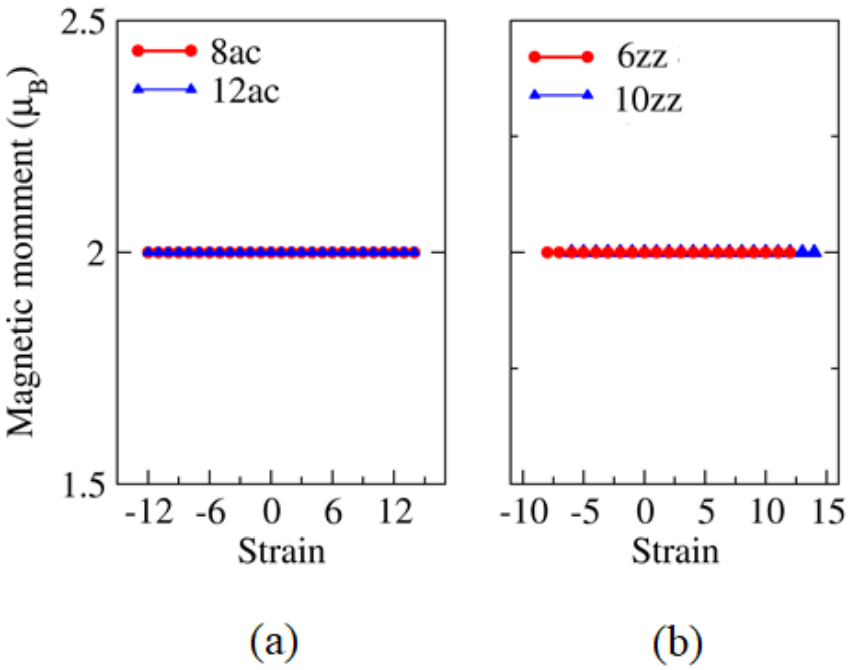

Figure S13: The magnetic momment (per VN pair) of edge hydrogenated (a) 8ac, 12ac and (b) 6zz, 10zz VNNRs at different strain condition.

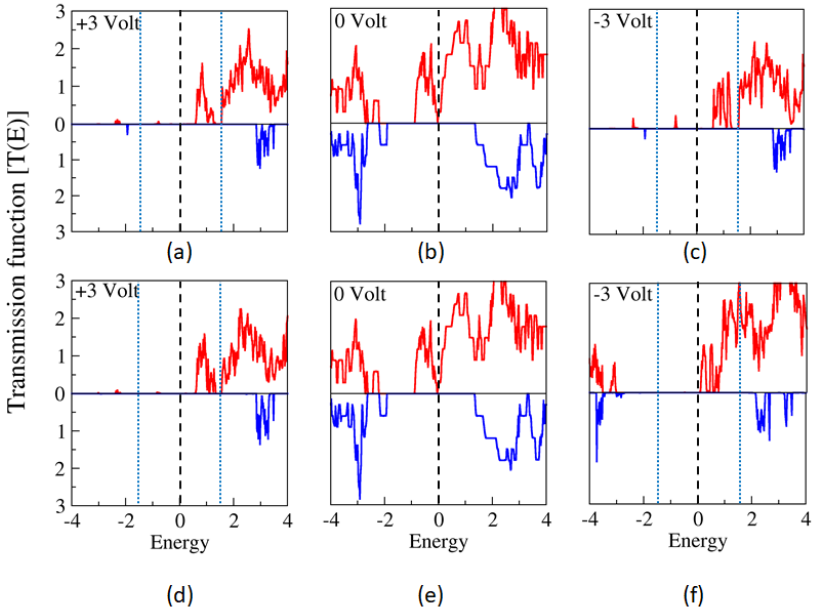

Figure S14: Spin resolved transmission functions at different bias voltage for (a - c) $L_1S_4R_1$ and (d - f) $L_1S_6R_1$ device system of edge hydrogenated 12ac VNNR. The blue dotted lines indicate the bias window ($-V_b/2$, $+V_b/2$). The Fermi energy is shown by black dotted line at zero energy.

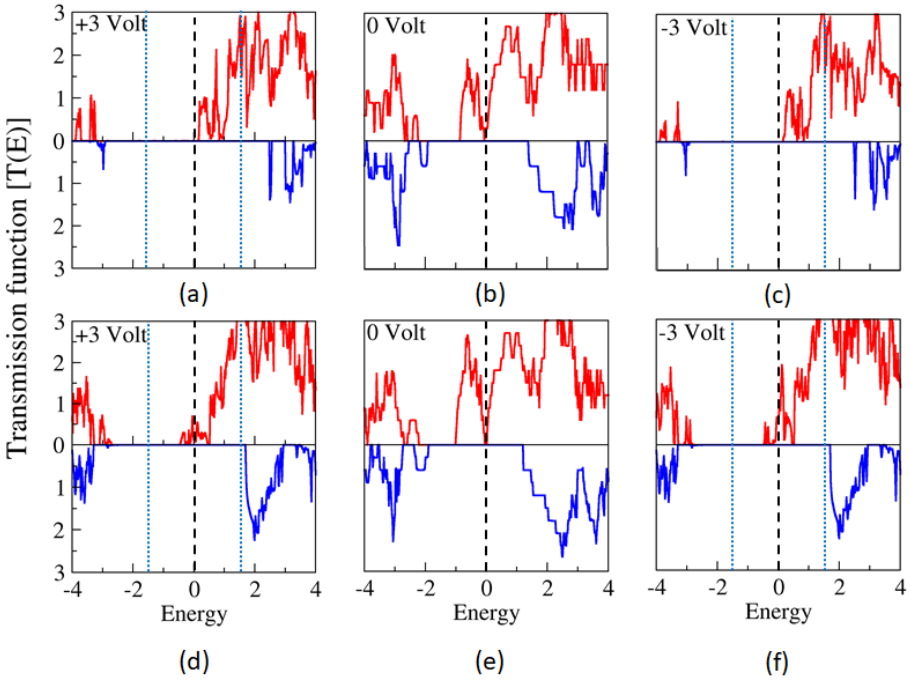

Figure S15: Spin resolved transmission functions of $L_1S_2R_1$ of edge hydrogenated 12ac VNNR at different bias voltage for (a - c) 4% tensile strain and (d - f) 4% compressive strain. The blue dotted lines indicate the bias window ($-V_b/2$, $+V_b/2$). The Fermi energy is shown by black dotted line at zero energy.

1 Modelling of VN composites

1.1 Using graphene substrate

To build ac-VN nanoribbon composite on graphene substrate, we have considered the lattice matching along ac-direction. The lattice constant of graphene along ac direction is 4.27 Å and 8ac VNNR is 5.53 Å. So, the lattice mismatch is near about 22.75%. To reduce this factor, we consider 4 unit cells of graphene (along ac direction) and 3 unit cells of 8ac VNNR to construct the unit cell of composite system. Here the lattice mismatch factor is reduced to 2.998%.

The interlayer distance in optimized 8ac VNNR/graphene composite is about 3.4 Å.

1.2 Using MoS_2 substrate

The lattice constant of edge hydrogenated 12ac VN is 5.53 Å and lattice constant of MoS_2 along ac direction is 5.48 Å. The latice mismatch factor in this case in only 0.99%. The lattice constant for edge hydrogenated 10zz VN is 3.169 Å and the lattice constant of MoS_2 along zz direction is 3.189 Å. The lattice mismatch in this case in only 0.6%. So, we can expect this type of composite modelling may give enough stablity. To account the van-der Waals interaction between VNNR and MoS_2 layer in VNNR/MoS_2 composites, DFT-D3 dispersion correction proposed by Grimme is used.[1,2] Keeping all the condition same with the previous calculation only the energy cut-off for the wavefunctions is reduced to 400 eV due to large number of atoms in the unit cell.

After optimization the lattice constant of 12ac VNNR/MoS_2 composite is 5.50 Å and the lattice constant of 10zz VNNR/MoS_2 composite 3.169 Å. The interlayer distance in both the composite is about 2.48 Å.

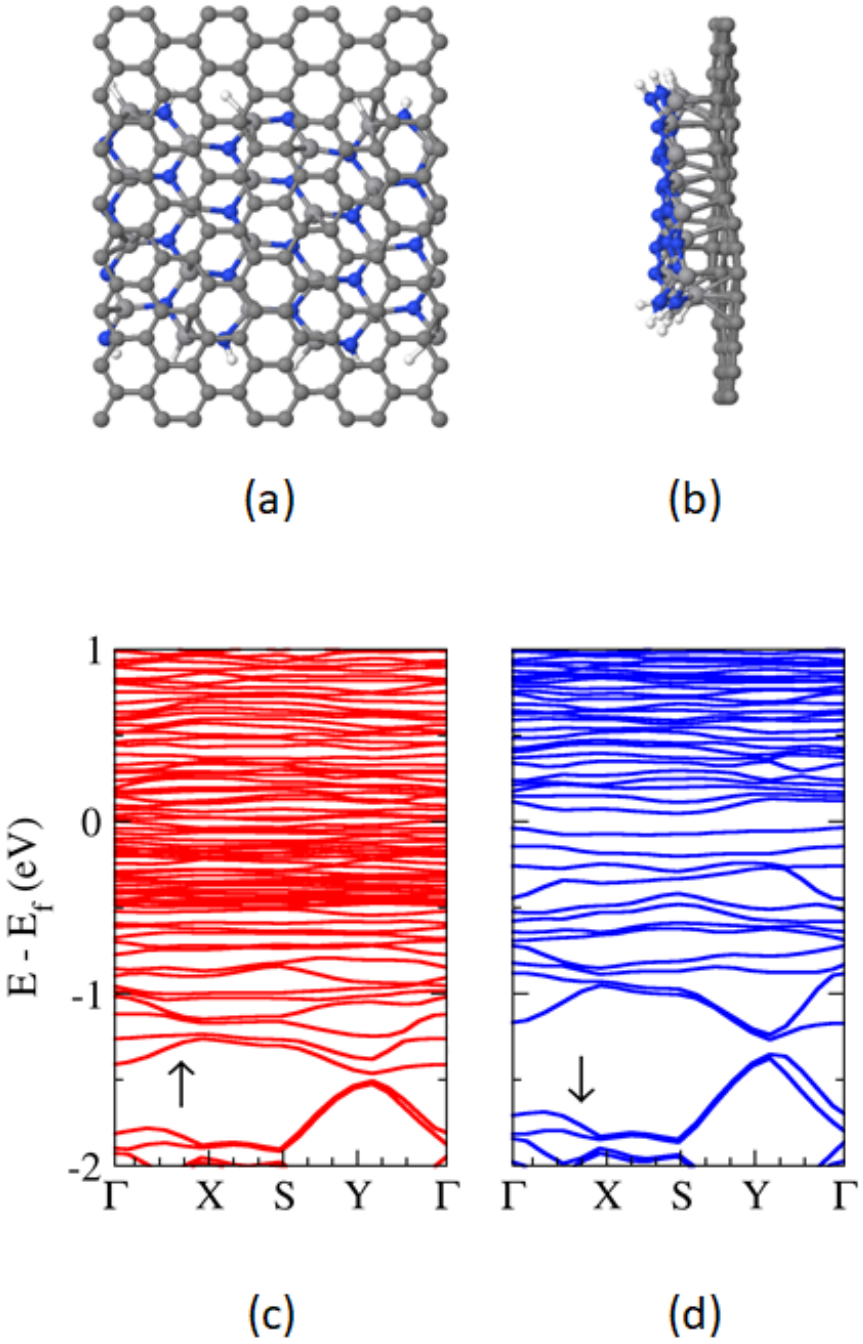

Figure S16: (a) Top view and (b) the side view of the edge hydrogenated 8-ac-VN/graphene composite.(c), (d) are the up spin and down spin band structure for the composite, respectively. Red curves signifies up spin (↑) where blue ones signifies down spin (↓). Fermi energy is shifted to zero.

Table S1: The energy difference between ferromagnetic and antiferromagnetic state of bare ac and zz VNNRs.

System	width(M)	$E_{fm} - E_{afm}$ (eV)
ac-NR	8	-0.8826
	12	-1.5978
	16	-1.8312
	20	-2.3216
zz-NR	6	-0.5160
	10	-1.1208
	14	-1.7591
	18	-2.1758

Table S2: The spin resolved band gaps for down spin channel of edge hydrogenated VN-NRs

System	width(M)	E_g (eV)
ac-NR	4	3.89
	8	3.96
	12	4.05
	16	4.20
	20	4.31
zz-NR	4	2.51
	6	2.63
	10	2.82
	14	2.92
	18	2.99

Table S3: The energy difference between ferromagnetic and antiferromagnetic state of edge hydrogenated ac and zz VNNRs at different strain.

System	width(M)	strain	$E_{fm} - E_{afm}$ (eV)
ac-NR	8	+14%	-0.7251
		+7%	-1.1680
		-6%	-1.0840
		-12%	-0.8080
	12	+14%	-1.8434
		+7%	-1.7915
		-6%	-1.6277
		-12%	-1.1560
zz-NR	6	+12%	-0.5308
		+6%	-0.6847
		-4%	-0.8290
		-8%	-0.9158
	10	+12%	-0.3190
		+6%	-1.1993
		-3%	-1.1411
		-6%	-2.3114

References

(1) Grimme, S. Density functional theory with London dispersion corrections. *Wiley Interdiscip. Rev. Comput. Mol. Sci.* **2011**, *1*, 211–228.

(2) Moellmann, J.; Grimme, S. DFT-D3 study of some molecular crystals. *J. Phys. Chem. C* **2014**, *118*, 7615–7621.